Title

Chemical shift assignments of a calmodulin intermediate with two Ca2+ bound in complex with the IQ-motif of voltage-gated Ca2+ channels (CaV1.2)

Journal

Biomolecular NMR Assignments, 13(1)

ISSN

1874-2718

Authors

Salveson, Ian
Anderson, David E
Hell, Johannes W
et al.

Publication Date

2019-04-01

DOI

10.1007/s12104-019-09883-0

Peer reviewed

HHS Public Access

Author manuscript

Biomol NMR Assign. Author manuscript; available in PMC 2020 April 01.

Published in final edited form as:

Biomol NMR Assign. 2019 April ; 13(1): 233–237. doi:10.1007/s12104-019-09883-0.

Chemical Shift Assignments of a Calmodulin Intermediate with Two Ca^{2+} Bound in Complex with the IQ-motif of Voltage-gated Ca^{2+} Channels ($Ca_V1.2$)

Ian Salveson[1], **David E. Anderson**[1], **Johannes W. Hell**[2], and **James B. Ames**[1,*]

[1]Department of Chemistry, University of California, Davis, CA 95616

[2]Department of Pharmacology, University of California, Davis, CA 95616

Abstract

Calcium-dependent inactivation (CDI) of neuronal voltage-gated Ca^{2+} channels ($Ca_V1.2$) is important for synaptic plasticity, which is associated with learning and memory. The Ca^{2+}-dependent binding of calmodulin (CaM) to $Ca_V1.2$ is essential for CDI. Here we report NMR assignments for a CaM mutant (D21A/D23A/D25A/E32Q/D57A/D59A/N61A/E68Q, called CaM^{EF12}) that contains two Ca^{2+} bound at the third and fourth EF-hands (EF3 and EF4) and is bound to the IQ-motif (residues 1644–1665) from $Ca_V1.2$ (BMRB accession no. 27692).

Keywords

calmodulin; EF-hand; $Ca_V1.2$; IQ-motif; synaptic plasticity; CDI

Biological Context

The neuronal L-type voltage-gated Ca^{2+} channel ($Ca_V1.2$) controls the excitability of the postsynaptic membrane in hippocampal neurons, which plays an important role in learning and memory (Hell et al, 1993; Moosmang et al, 2005; Vogl et al, 2015). The cytosolic C-terminal region of $Ca_V1.2$ (residues 1644–1665, called IQ-motif) is important for promoting Ca^{2+}-dependent inactivation (CDI) of $Ca_V1.2$ (Erickson et al, 2001; Zuhlke et al, 1999). Ca^{2+}-saturated CaM (with 4 Ca^{2+} bound) binds tightly to the IQ-motif (Findeisen et al, 2013), and the $Ca_V1.2$ mutation I1654A that disables Ca^{2+}/CaM binding also prevents CDI (Ben Johny et al, 2013). The Ca^{2+}-free form of calmodulin (apoCaM) has been suggested to bind to $Ca_V1.2$ under basal conditions, which may explain how $Ca_V1.2$ is pre-associated with CaM (Adams et al, 2014). Atomic resolution structures are currently known for the IQ-motif bound to both apoCaM (Gabelli et al, 2014) and Ca^{2+}-saturated CaM (Van Petegem et al, 2005), but no structural information is known for the IQ-motif bound to the half-saturated intermediate state of CaM (with Ca^{2+} bound at EF3 and EF4 but not bound at EF1 and EF2). This CaM intermediate state is functionally present under basal conditions (Wang et al, 2018) and may play a role in CDI (Simms & Zamponi, 2014). To study the structure of the half-saturated CaM intermediate state, we first constructed a mutant protein (D21A/D23A/

*To whom correspondence should be addressed: jbames@ucdavis.edu.

D25A/E32Q/D57A/D59A/N61A/E68Q, called CaM^{EF12}) that disables Ca^{2+} binding to EF1 and EF2 but retains Ca^{2+}-binding solely at EF3 and EF4. This CaM intermediate state is also important for regulation of ryanodine receptors (Sondergaard et al, 2015) and nitric oxide synthase (Piazza et al, 2016). We report detailed NMR resonance assignments for the CaM^{EF12} mutant with two Ca^{2+} bound (called $Ca^{2+}{}_2/CaM^{EF12}$) that is bound to the IQ-motif of $Ca_V1.2$ (the complex is called $Ca^{2+}{}_2/CaM^{EF12}$-IQ) as a first step toward solving the structure of this complex.

Methods and Experiments

Preparation of $Ca^{2+}{}_2/CaM^{EF12}$ bound to the $Ca_V1.2$ IQ-motif.

A cDNA of *Homo sapiens* calmodulin that contained the mutations (D21A/D23A/D25A/E32Q/D57A/D59A/N61A/E68Q) was subcloned into pET-11b vector (Novagen) that produced recombinant CaM^{EF12} without any affinity tag or extra residues. Uniformly ^{15}N-labeled and ^{13}C,^{15}N-labeled CaM^{EF12} were expressed in bacterial cells grown on M9 minimal media supplemented with ^{15}N-labeled NH_4Cl (0.5 g per liter of cell culture) and ^{13}C-labeled glucose (3 g per liter). The recombinant CaM^{EF12} protein was purified using Ca^{2+}-dependent hydrophobic interaction chromatography (Gopalakrishna & Anderson, 1982). A peptide fragment of the $Ca_v1.2$ IQ-motif (residues 1642–1665) was purchased from GenScript, dissolved in DMSO-d_6 and quantified using UV-Vis absorption. A 1.5-fold excess of $Ca_v1.2$ IQ-motif was added to Ca^{2+}-bound CaM^{EF12} and the complex ($Ca^{2+}{}_2/CaM^{EF12}$-IQ) was subsequently concentrated to 500 μM in the presence of 2 mM $CaCl_2$ using a 3K Amicon concentrator.

NMR spectroscopy.

Samples of $Ca^{2+}{}_2/CaM^{EF12}$-IQ complex for NMR analysis were prepared by exchanging the protein complex into a buffer containing 20 mM Tris-d_{11} (pH 7.5) with 1 mM $CaCl_2$, and 92% H_2O/8% D_2O. All NMR experiments were performed at 303K on a Bruker Avance 800 MHz spectrometer equipped with a four channel interface and triple resonance cryogenic (TCI) probe. The ^{15}N-^{1}H HSQC spectrum (Fig. 1) was recorded with 256 × 2048 complex points for ^{15}N(F1) and ^{1}H(F2), respectively. Assignment of backbone resonances was obtained by analyzing the following spectra: HNCA, HNCACB, CBCA(CO)NH, HNCO (Ikura et al, 1990). Side chain resonances were assigned by analyzing HCCH-TOCSY (Ikura et al, 1991). The NMR data were processed using NMRPipe (Delaglio et al, 1995) and analyzed using Sparky NMRFAM (Lee et al, 2015).

Assignments and Data Deposition

A two-dimensional ^{15}N-^{1}H HSQC NMR spectrum of $Ca^{2+}{}_2/CaM^{EF12}$ bound to unlabeled $Ca_v1.2$ IQ peptide illustrates representative NMR assignments (Fig. 1). NMR assignments were based on 3D heteronuclear NMR spectra recorded from ^{13}C/^{15}N-labeled $Ca^{2+}{}_2/CaM^{EF12}$ bound to unlabeled IQ peptide (residues 1642–1665). The NMR spectra of $Ca^{2+}{}_2/CaM^{EF12}$-IQ exhibited well-dispersed peaks with uniform intensities indicative of a stably folded protein complex. A few amide resonances exhibit noteworthy downfield shifts, including T29, I101, and N138 that are each located in β-strands (see arrows in Fig. 2) and

are expected to form antiparallel β-sheets with strong backbone amide hydrogen bonds. Two downfield peaks assigned to G99 (EF3) and G135 (EF4) are likely caused by a strong hydrogen bond between the backbone NH of G99 and G135 with the side chain carboxyl group of D94 and D130, respectively caused by Ca^{2+} binding to EF3 and EF4. The absence of corresponding downfield shifts for G26 (EF1) and G62 (EF2) is consistent with a lack of Ca^{2+} binding at EF1 and EF2. More than 92% of the main chain ^{13}C resonances ($^{13}C\alpha$, $^{13}C\beta$, and ^{13}CO), 90% of backbone amide resonances (^{1}HN, ^{15}N), and 74% of methyl side chain resonances were assigned. The unassigned residues (14–15, 30–32, 43, 59–61, 75, 78, 94) had overlapped backbone amide resonances and/or weak NMR intensities that obscured their assignment. In particular, the EF-hand loop residues in EF1 (residues 30–32) and EF2 (residues 58–61) could not be assigned due to weak NMR intensities, perhaps caused by conformational disorder in these Ca^{2+}-free binding loops. A complete listing of the chemical shift assignments (^{1}H, ^{15}N, ^{13}C) of $Ca^{2+}{}_2/CaM^{EF12}$ bound to unlabeled $Ca_v1.2$ IQ peptide have been deposited in the BioMagResBank (http://www.bmrb.wisc.edu) under accession number 27692.

The secondary structure of $Ca^{2+}{}_2/CaM^{EF12}$ in the complex was calculated based on the chemical shift index (Wishart et al, 1992) of each assigned amino acid residue and ANN-secondary structure prediction using TALOS (Shen et al, 2009) (Fig. 2). As expected, $Ca^{2+}{}_2/CaM^{EF12}$ contains four EF-hands comprised of eight α-helices. The helices are named α1 (residues 8–20), α2 (residues 30–39), α3 (residues 46–56), α4 (residues 66–76), α5 (residues 83–93), α6 (residues 103–113), α7 (residues 119–129) and α8 (residues 139–146) depicted by blue rectangles in Fig. 2. In addition, a short and conserved β-strand was observed in EF1 (residues 27–29), EF2 (residues 63–65), EF3 (residues 100–102) and EF4 (residues 136–138) shown by orange arrows in Fig. 2. The overall secondary structure of $Ca^{2+}{}_2/CaM^{EF12}$ is similar to that observed in the crystal structure of Ca^{2+}-saturated CaM bound to IQ peptide (Van Petegem et al, 2005). A plot of the amide chemical shift perturbation caused by the binding of the IQ peptide reveals that CaM^{EF12} residues in the N-terminal domain (residues 1–80 in EF1 and EF2) exhibit relatively small chemical shift differences (CSDs) upon binding to the IQ peptide (Fig. 3). In stark contrast, the CaM residues in the C-terminal domain (residues 81–149) exhibit much larger CSDs induced by IQ binding (Fig. 3). The larger CSD values for the C-terminal domain residues suggest that the IQ-motif is bound to the C-terminal domain (EF3 and EF4). The relatively smaller CSD values for the N-terminal domain residues suggest that the IQ peptide may not make contact with the CaM N-terminal domain (EF1 and EF2), in contrast to what is seen in the crystal structure of Ca^{2+}-saturated CaM bound to IQ. The NMR assignments of $Ca^{2+}{}_2/CaM^{EF12}$ bound to the CaV1.2 IQ-motif presented here are an important first step toward determining the full three-dimensional structure of $Ca^{2+}{}_2/CaM^{EF12}$ bound to $Ca_V1.2$.

Acknowledgements

We thank Jeff Walton for technical support and help with NMR experiments. Work supported by NIH grants (EY012347) to J.B.A and (AG055357) to J.W.H.

References

Adams PJ, Ben-Johny M, Dick IE, Inoue T, Yue DT (2014) Apocalmodulin itself promotes ion channel opening and Ca(2+) regulation. Cell 159: 608–622 [PubMed: 25417111]

Ben Johny M, Yang PS, Bazzazi H, Yue DT (2013) Dynamic switching of calmodulin interactions underlies Ca2+ regulation of CaV1.3 channels. Nature communications 4: 1717

Delaglio F, Grzesiek S, Vuister GW, Zhu G, Pfeiffer J, Bax A (1995) NMRPipe: a multidimensional spectral processing system based on UNIX pipes. J Biomol NMR 6: 277–293 [PubMed: 8520220]

Erickson M, Alseikhan B, Peterson B, Yue D (2001) Preassociation of calmodulin with voltage-gated Ca(2+) channels revealed by FRET in single living cells. Neuron 31: 973–985 [PubMed: 11580897]

Findeisen F, Rumpf CH, Minor DL, Jr. (2013) Apo states of calmodulin and CaBP1 control CaV1 voltage-gated calcium channel function through direct competition for the IQ domain. Journal of molecular biology 425: 3217–3234 [PubMed: 23811053]

Gabelli SB, Boto A, Kuhns VH, Bianchet MA, Farinelli F, Aripirala S, Yoder J, Jakoncic J, Tomaselli GF, Amzel LM (2014) Regulation of the NaV1.5 cytoplasmic domain by calmodulin. Nature communications 5: 5126

Gopalakrishna R, Anderson WB (1982) Ca2+-induced hydrophobic site on calmodulin: application for purification of calmodulin by phenyl-Sepharose affinity chromatography. Biochem Biophys Res Commun 104: 830–836 [PubMed: 6803791]

Hell JW, Westenbroek RE, Warner C, Ahlijanian MK, Prystay W, Gilbert MM, Snutch TP, Catterall WA (1993) Identification and differential subcellular localization of the neuronal class C and class D L-type calcium channel alpha 1 subunits. J Cell Biol 123: 949–962 [PubMed: 8227151]

Ikura M, Kay LE, Bax A (1990) A novel approach for sequential assignment of 1H, 13C, and 15N spectra of proteins: heteronuclear triple-resonance three-dimensional NMR spectroscopy. Application to calmodulin. Biochemistry 29: 4659–4667 [PubMed: 2372549]

Ikura M, Spera S, Barbato G, Kay LE, Krinks M, Bax A (1991) Secondary structure and side-chain 1H and 13C resonance assignments of calmodulin in solution by heteronuclear multidimensional NMR spectroscopy. Biochemistry 30: 9216–9228 [PubMed: 1909892]

Lee W, Tonelli M, Markley JL (2015) NMRFAM-SPARKY: enhanced software for biomolecular NMR spectroscopy. Bioinformatics 31: 1325–1327 [PubMed: 25505092]

Moosmang S, Haider N, Klugbauer N, Adelsberger H, Langwieser N, Muller J, Stiess M, Marais E, Schulla V, Lacinova L, Goebbels S, Nave K, Storm D, Hofmann F, Kleppisch T (2005) Role of hippocampal Cav1.2 Ca2+ channels in NMDA receptor-independent synaptic plasticity and spatial memory. The Journal of neuroscience : the official journal of the Society for Neuroscience 25: 9883–9892 [PubMed: 16251435]

Piazza M, Dieckmann T, Guillemette JG (2016) Structural Studies of a Complex Between Endothelial Nitric Oxide Synthase and Calmodulin at Physiological Calcium Concentration. Biochemistry

Shen Y, Delaglio F, Cornilescu G, Bax A (2009) TALOS+: a hybrid method for predicting protein backbone torsion angles from NMR chemical shifts. J Biomol NMR 44: 213–223 [PubMed: 19548092]

Simms BA, Zamponi GW (2014) Neuronal voltage-gated calcium channels: structure, function, and dysfunction. Neuron 82: 24–45 [PubMed: 24698266]

Sondergaard MT, Tian X, Liu Y, Wang R, Chazin WJ, Chen SR, Overgaard MT (2015) Arrhythmogenic Calmodulin Mutations Affect the Activation and Termination of Cardiac Ryanodine Receptor-mediated Ca2+ Release. J Biol Chem 290: 26151–26162 [PubMed: 26309258]

Van Petegem F, Chatelain FC, Minor DL, Jr.(2005) Insights into voltage-gated calcium channel regulation from the structure of the CaV1.2 IQ domain-Ca2+/calmodulin complex. Nature structural & molecular biology 12: 1108–1115

Vogl AM, Brockmann MM, Giusti SA, Maccarrone G, Vercelli CA, Bauder CA, Richter JS, Roselli F, Hafner AS, Dedic N, Wotjak CT, Vogt-Weisenhorn DM, Choquet D, Turck CW, Stein V, Deussing JM, Refojo D (2015) Neddylation inhibition impairs spine development, destabilizes synapses and deteriorates cognition. Nature neuroscience 18: 239–251 [PubMed: 25581363]

Wang K, Holt C, Lu J, Brohus M, Larsen K, Overgaard M, Wimmer R, Van Petegem F (2018) Arrhythmia mutations in calmodulin cause conformational changes that affect interactions with the cardiac voltage-gated calcium channel. Proceedings of the National Academy of Sciences of the United States of America 115: E10556–E10565 [PubMed: 30348784]

Wishart DS, Sykes BD, Richards FM (1992) The chemical shift index: a fast and simple method for the assignment of protein secondary structure through NMR spectroscopy. Biochemistry 31: 1647–1651. [PubMed: 1737021]

Zuhlke RD, Pitt GS, Deisseroth K, Tsien RW, Reuter H (1999) Calmodulin supports both inactivation and facilitation of L-type calcium channels. Nature 399: 159–162 [PubMed: 10335846]

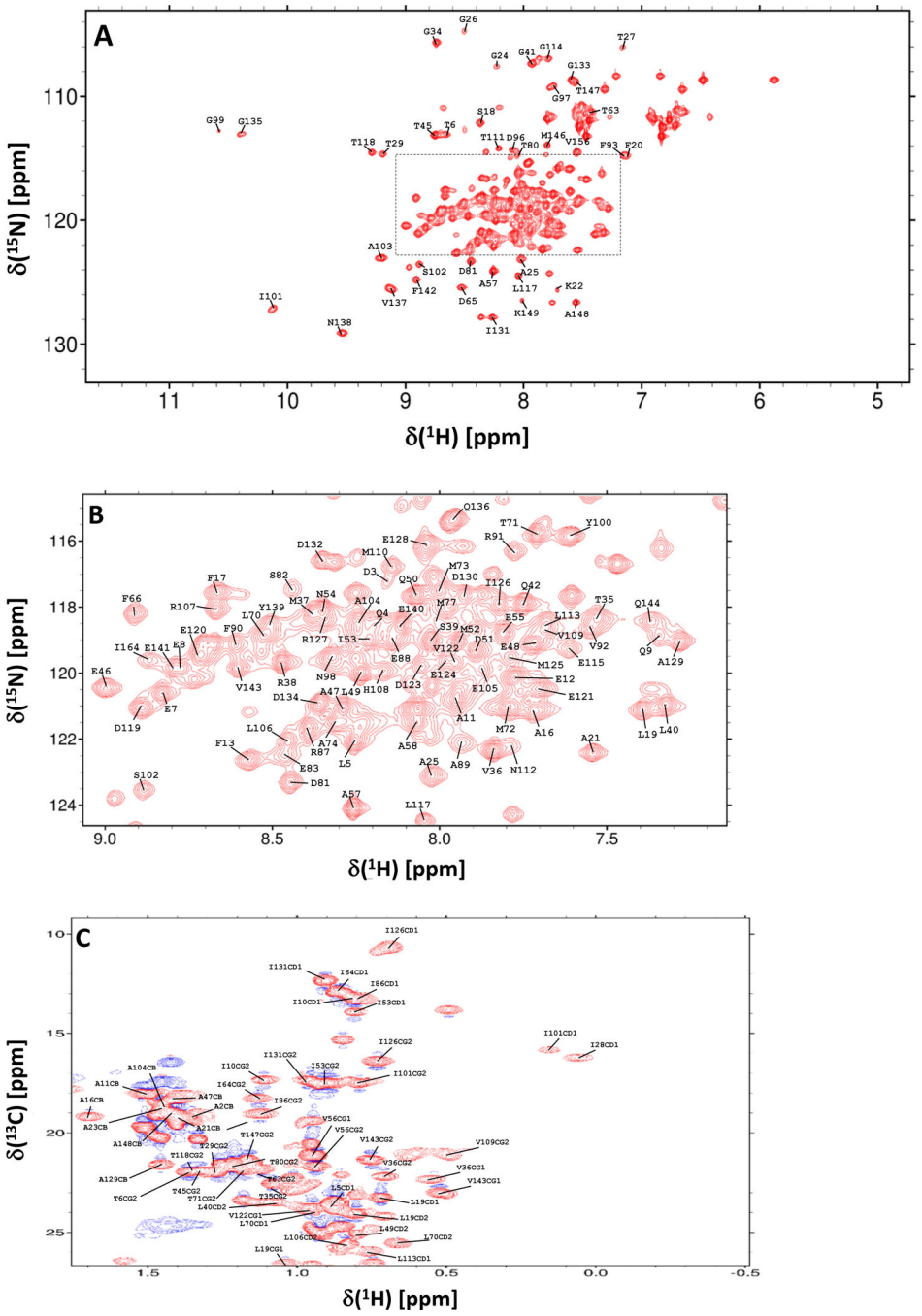

Fig. 1:

Two-dimensional ^{15}N-^{1}H HSQC NMR spectrum of ^{15}N-labeled $Ca^{2+}{}_2$/CaM^{EF12} bound to unlabeled Ca_v1.2 IQ peptide at pH 7.5 recorded at 800-MHz ^{1}H frequency (A). Expanded view of the crowded spectral region in the center of the spectrum (B). Constant-time ^{13}C-^{1}H HSQC spectrum of 13C-labeled $Ca^{2+}{}_2$/CaM^{EF12} bound to unlabeled Ca_v1.2 IQ peptide (C). Representative assignments are indicated; complete assignments are available as BMRB accession no. 27692.

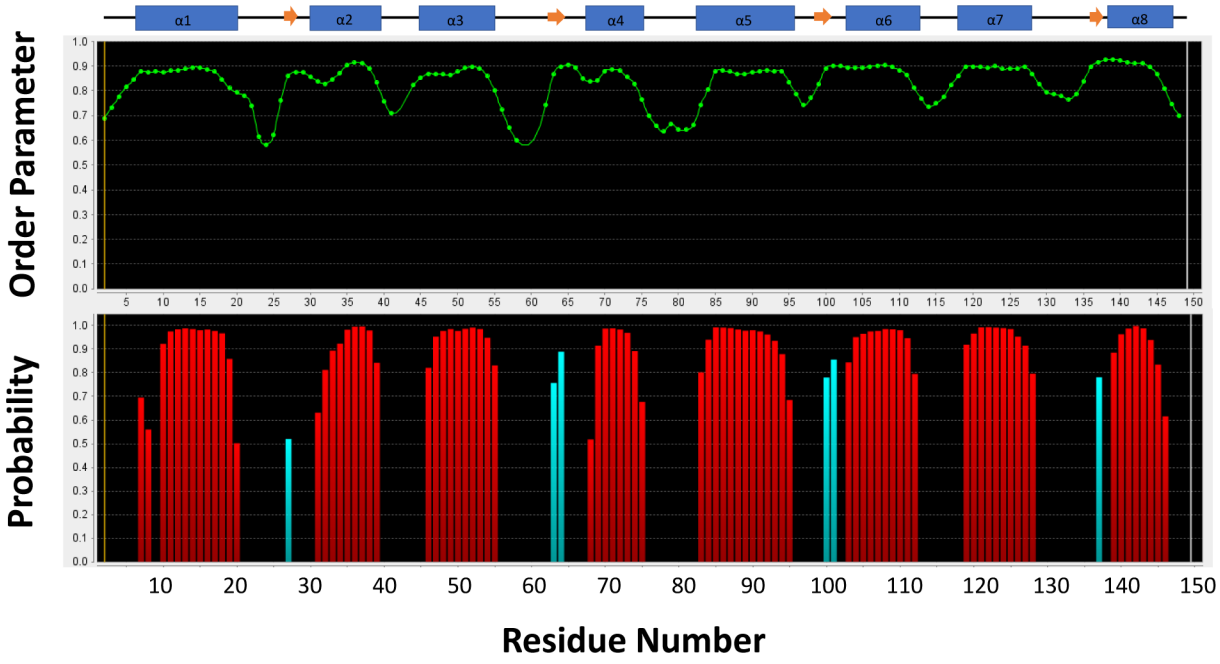

Fig. 2:

Secondary structure of $Ca^{2+}{}_2$/CaM^{EF12} bound to $Ca_v1.2$ IQ. Normalized order parameter (upper panel) and ANN-secondary structure probability (lower panel) plotted as a function of residue number. Secondary structure elements (rectangle for helix and arrow for β-strand) were calculated on the basis of chemical shift index and sequential NOE patterns.

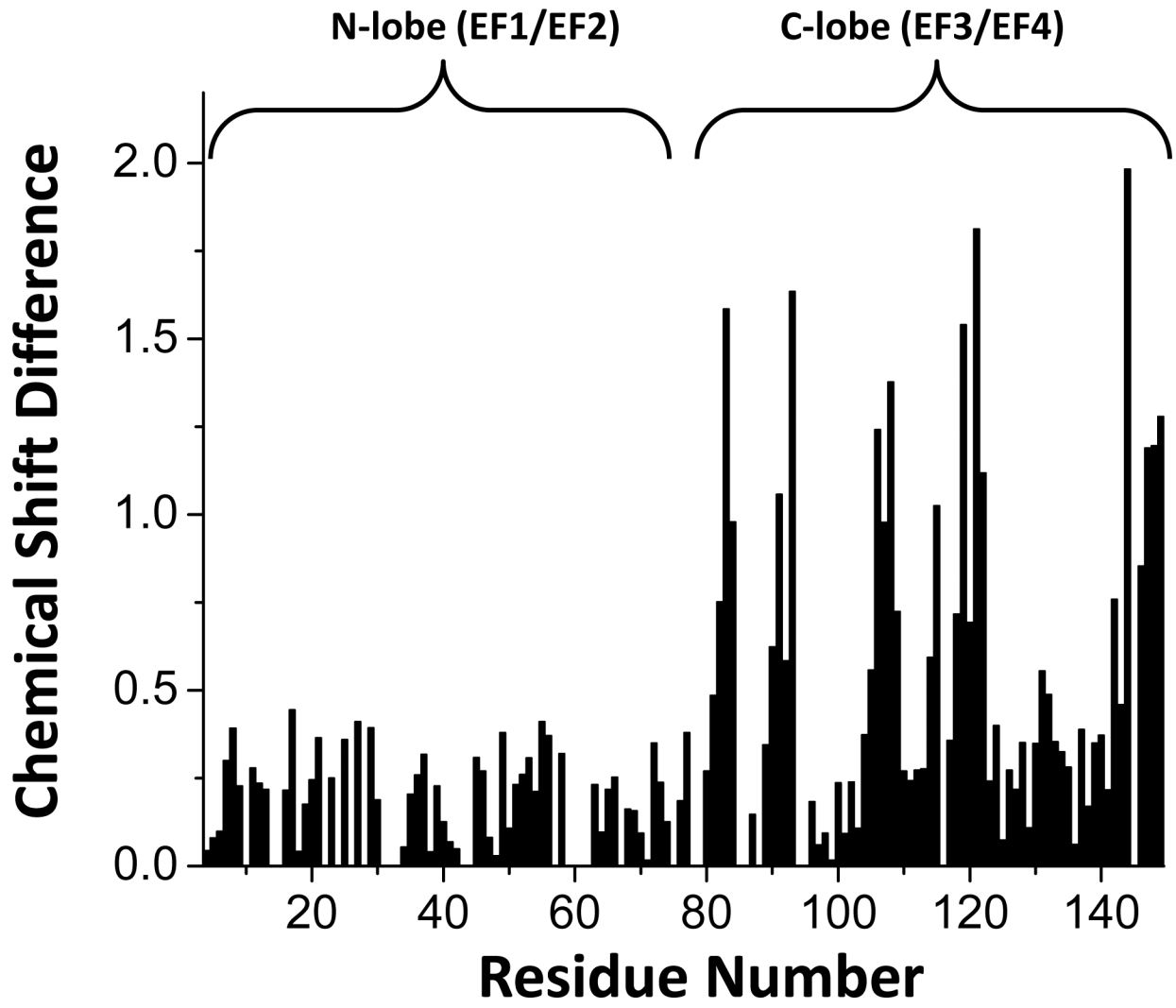

Fig. 3:

Amide chemical shift perturbation for $Ca^{2+}{}_2$/CaM^{EF12} in the presence versus absence of bound IQ peptide. The chemical shift difference (CSD) was calculated as (CSD = $\{(HN_A - HN_B)^2 + (^{15}N_A - ^{15}N_B)^2\}^{1/2}$ HN_A and HN_B are amide proton chemical shift of $Ca^{2+}{}_2$/CaM^{EF12} in the presence and absence of IQ peptide respectively, and $^{15}N_A$ and $^{15}N_B$ are amide ^{15}N chemical shift of $Ca^{2+}{}_2$/CaM^{EF12} in the presence and absence of IQ peptide respectively. Chemical shift assignments for $Ca^{2+}{}_2$/CaM^{12} (without IQ) were derived from wildtype apo-CaM (BMRB 27190) for N-terminal domain residues (1–79) and from wild type Ca^{2+}-saturated CaM (BMRB 547) for the C-terminal domain residues (80–149). The CSD values of the mutated residues in EF1 and EF2 (21, 23, 25, 57, 59, and 61) are not meaningful (due to the mutation) and are not shown.